Journal of Asian Concrete Federation

journal homepage: https://jacf.sfulib3.publicknowledgeproject.org/index.php/jacf

Passivation and Corrosion Behavior of TF400 in Simulated Concrete Pore Solution

Tao Xing [a]* Jiayue Lu[a] Fei Guo[a]

[a]. State Key Laboratory of High Performance Civil Engineering Materials, Nanjing 210008, China;
[b]. Jiangsu Sobute New Materials Co., Ltd, Nanjing, PR China

A B S T R A C T

In simulated concrete pore solution, passivation and corrosion behavior of TF400 titanium alloy (TF) and Common steel (CS) were investigated, with testing methods of electrochemical techniques and micro morphology. The results show that both TF and common steel bar can form adherent, compact and protective passive film on surface, improving the corrosion resistance. The polarization resistance (Rp) of titanium alloy is $10^6\Omega.cm^2$, which is three orders of magnitude of that of common steel bar ($10^3\Omega.cm^2$). When in a completely passivated state, the passive film resistance (Rf) of TF is $2\times10^5\Omega.cm^2$, and that of CS is $2\times10^4\Omega.cm^2$. TF400 titanium alloy exhibit superior corrosion resistance when exposed to high concentration of chlorine. The corrosion current density (Icorr) of TF is basically stable at 10^{-7} A/cm^2 and the Rp maintained at $10^5\Omega.cm^2$. As comparison, the Icorr of CS is 10^{-4} A/cm^2 and the Rp is $10^3\Omega.cm^2$. Whether the passivation performance or corrosion resistance, TF is far superior to CS, and can replace CS in marine concrete structures.

Keywords: TF400 titanium alloy; simulated concrete pore solution; corrosion current density;polarization resistance.

1. Introduction

With the development and utilization of marine resources, reinforced concrete has been widely used in marine engineering constructions. However, Portland cement concrete is easily destroyed under aggressive sea water, which shorten the actual service life of current concrete constructions. Chloride-induced corrosion of reinforced concrete is considered as the most destructive factor[1, 2], the destruction mechanism of reinforced concrete is mainly accused by the corrosion of steel bar in the presence of chloride ion. Herein, the stability of steel bar is a key factor of reinforced concrete under marine condition[3, 4].

Under high alkaline environments, the redox reaction takes place on the surface of steel bar and forms a dense oxide film, which is the passive film. This protective passive film can protect metallic matrix from corrosion ions and improve the corrosion resistance of steel[5, 6], which can prolong the service life of reinforced concrete structures. Therefore, the properties of oxide film have important impacts on the performance of reinforced concrete. So far, the composition and property of passive film of carbon steel under alkaline environment have been widely investigated and a series of theories have been proposed [7-11]. Ohtsuka et al. [12] studied the corrosion phenomenon by knowledge of electrochemical and electrochemical measurement techniques. The process of passivation and corrosion of reinforcement can be detected by testing the electrochemical parameters. The characters and compositions of passive film can be observed by SEM, coupled with X-ray photoelectron spectroscopy (XPS) and raman spectroscopy [13-16].

In high chloride environment, passive film of carbon steel would be corrode and destroyed, which will lead to the local corrosion and pitting corrosion. Therefore, carbon steel is not suitable to be used in reinforced concrete structure under marine environment because of its poor corrosion resistance [17-19]. Consequently, it is important to seek a new high corrosion resistant material to improve the service life of reinforced concrete under marine environment. In recent years, titanium alloys have been proposed to use in

* Corresponding author: Tao Xing (xingtao@cnjsjk.cn)

DOI http://dx.doi.org/10.18702/acf.2026.12.3.47

Received: 25-May-2026; Revised: 03-Jul-2026; Accepted: 09-Jul-2026; Published online: 31-Jul-2026

ISSN 2465-7964, eISSN 2465-7972.

marine engineering because of its low density, high strength and excellent corrosion resistance. Numerous studies on the performance of passivation and corrosion of titanium alloys have been performed in recent years. The high corrosion resistance of titanium alloys is mainly owning to the protective oxidation film on its surfaces, which protects the surface from corrosion by corrosive ions [20, 21]. The composition the passive film of titanium alloy was investigated and oxide layer is mainly TiO_2, containing small amounts of TiO and Ti_2O_3 with potential of -0.75V [22-25]. In chlorine environment, the main corrosion forms of titanium alloy are pitting corrosion and crevices corrosion. Titanium alloy can exhibits good corrosion resistance in corrosive Cl- solution in the concentration of is 0.5 mol/L or 1.5 mol/L. Zhang et al. [26] claimed that Ti-xFe-B (Ti-Fe) alloys not only have the similar strength with carbon steel, but show much higher corrosion resistance than that of carbon steel. Because of iron can play a role of solution strengthening during cooling and improve the abrasive resistance and corrosion resistance of alloy. When the iron content reaches 5%, the values of tensile strength of the Ti-Fe alloy increases to 834 MPa.

Ti-3Fe-0.1B (TF400) is an alloy of Ti-Fe, which has been proven to have good mechanical properties in laboratory[27]. However, the behavior of corrosion and properties of passivation have not been detailed studied yet. In this work, the passivation and corrosion behaviors of TF400 (TF) and carbon steel (CS) were studied in simulated concrete pore solution to investigate the passivation and corrosion performance of TF400. Passivation and corrosion resistance properties were monitored by AC impedance spectroscopy and linear polarization curve. The composition and microstructure of TF was investigated with SEM and EDS.

2. Experimental

2.1. Materials

The steel bars used in this study were commercial 45 carbon steel and TF400 alloy. The compositions of carbon steel and TF400 were show in table 1. Samples were cut into dimension of ø 12mm × 20mm (shown in Fig. 1a). One side of the steel bar acted as the working surfaces and the other side was junction surface. The specimens were connected with copper wire soldered and embedded in epoxy resin, leaving only one working surface with the area of 1.13 cm^2. Prior to the tests, the surface of all samples was polished with SiC papers (from garde 240-7000), and then cleaned with alcohol and acetone. The polished working electrode was immersed in simulated concrete pore solution to conduct passivation test. The composition of simulated solution were mixed by $Ca(OH)_2$, NaOH and KOH with a pH of 13.2 [28]. Corrosion solution was prepared by adding different proportion of sodium chloride on the basis of simulated passivation solution, which is shown in Table 2. The concentrations of chloride ions in corrosion solution were 3.5wt% (0.598mol/L), 5.0wt% (0.855mol/L) and 7.0% (1.196mol/L) respectively.

Table 1. Actual composition (wt.%) of the TF400 alloy and 45 carbon steel.

Sample	B	N	O	C	Si	Mn	Ni	Ti	Fe
TF400 titanium alloy	0.1	0.01	0.079	0.016	-	-	-	Bal	3.36
45 carbon steel	-	-	-	0.43	0.23	0.58	0.03	-	Bal

Table 2. Chemical composition (mol/L) of passivation solution.

	KOH	NaOH	Ca (OH)2	NaCl
Passivation solution	0.6	0.2	sat	0
	0.6	0.2	sat	0.598
Corrosion solution	0.6	0.2	sat	0.855
	0.6	0.2	sat	1.196

2.2 Methods

2.2.1 Electrochemical measurements

CHI760E electrochemical workstation was used to conduct the electrochemical measurements. The schematic diagrams of testing specimens and three electrodes measuring system were shown in Fig. 1b. The steel bars were acted as the working electrode (WE), while a saturated calomel electrode (SCE) was used as reference electrode and a graphite flake was used as counter electrode (CE) with an area of 1.5 cm^2. All electrochemical measurements were conducted in simulated concrete pore solution.

Every electrochemical test needed to be performed under the condition that the value of open circle potential (OCP) was

relatively stable. The system was regarded as stabilize when the OCP value changed at 2 mV/min. Open circuit potential is a thermodynamic parameter, relating to the corrosion current density. The OCP value of reinforcement was tested firstly with testing time of 900s. The polarization curve and impedance spectrum can be measured according to the value of OCP. The polarization curve can reveal cathodic polarization curve and anodic polarization curve [29]. When linear polarization curve (LPC) is tested, the anode polarization curve and cathode polarization curve are tested simultaneously. Therefore, the initial potential and final potential are ±200 mV of OCP. The ESI was tested with a wide frequency ranged from 0.01 Hz to 10^5 Hz. The impedance curves were fitted by ZsimpWin software.

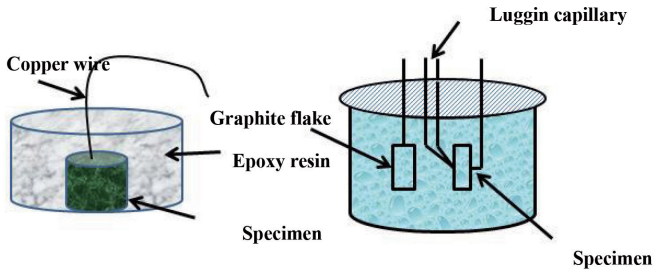

a b

Fig. 1. The diagram of electrochemical test specimens (a) and illustration of three electredes system used (b)

2.2.2. Surface composition and morphology

A Rigaku 3000 A diffractometer with CuKa radiation source was used to characterize the composition of oxide film on the surface of steel rebar. Accelerating voltage and accelerating current of the tests were 40 kV and 35 mA, respectively. Morphology of passive film was studied by scanning electron spectroscopy coupled with energy dispersive microscopy (SEM-EDS).

3. Results and Discussion

3.1 Open circuit potential evolution during passivation ages

The OCP values of TF and CS during passivation process were represented in Fig. 2. It can be seen from Fig. 2 that the OCP values of TF increased sharply in the early stage and then gradually stabilized at about -0.25 VSCE. After 3 days of passivation, the OCP value of TF increased slowly and tended to be stable at -0.15 V_{SCE}. As a comparison, the OCP value fluctuated greatly of CS in the initial stage. After 6 days, the OCP was basically stable about -0.17 V_{SCE}. That is because that the redox reaction on the surface of TF is intense and the passivation film is formed quickly in the early passivation period. As the passivation film is formed, the corrosion resistance of reinforcement increases and the OCP value becomes stable [30]. The OCP values of TF were higher than that of CS, indicating that the passivability of TF was superior to CS. This is attributed to that chromium can improve the passivation property of TF [31].

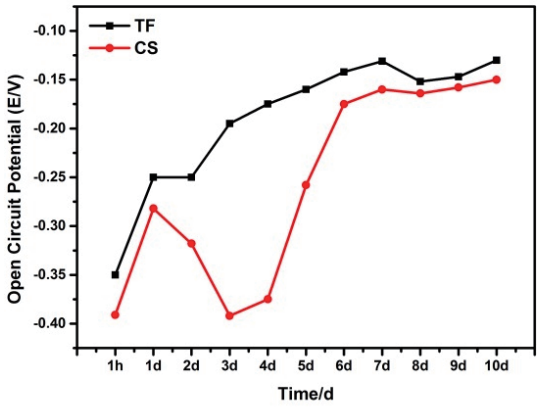

Fig. 2 volution of open-circuit potential of specimens immersed in simulated concrete pore solution.

3.2 Potentiodynamic polarization curve of passivation system

The linear polarization curves of TF and CS were shown in Fig. 3. It is observed that all cathodic polarization curves were basically coincident, which is owning to that all samples have the same cathode reaction in simulated solution and correspond to the following reaction [31]:.

$$O_2+4e^- + 2H_2O \rightarrow 4OH^- \quad (1)$$

With passivation ages extension, the polarization curves of CS and TF shifted to positive and stabled between -0.2 V_{SCE} and -0.1 V_{SCE} respectively. The breakdown potentials of passive film of CS and TF were approximately -0.1 V_{SCE} after completely passivation. The passive current densities of CS and TF were about 10^{-5} A/cm^2 10^{-7} A/cm^2 respectively. As shown in Fig. 3(a), the corrosion potentials of CS were about -0.3 V_{SCE} after passivation for 3 to 6 days, while the corrosion potentials were concentrated around -0.2 V_{SCE} after passivating for 7 to 10 days. From Fig. 3(b), all polarization curves had obvious passivation areas except for the 1 h sample, and the corrosion potentials were concentrated between -0.2 V_{SCE} and -0.1 V_{SCE} after passivating for 3 days. It is concluded that TF and CS can be passivated in simulated concrete pore solution, and the passivation rate of TF is higher than that of CS.

Corrosion current density (I_{corr}) and polarization resistance (R_p) of TF and CS were calculated by the polarization curve and shown in table.3. The Icorr value of TF reduced gradually from 3.5×10^{-6} A/cm^2 to the minimum value of 1.7×10^{-8}A/cm^2. At the same time, the Rp enlarged form $2.8\times10^3\Omega$.cm^2 to the maximum value of $1.9\times10^6\Omega$.cm^2. As a comparison, the Icorr of CS decreased from 4.9×10^{-4} A/cm^2 to 3.5×10^{-6} A/cm^2, and the Rp increased from 5.7×10^2 Ω.cm^2 to 6.8×10^4 Ω.cm^2. By comparing the values of Icorr and Rp of CS and TF at various ages of passivation, it can be seen that the passivability and corrosion resistance of TF are much better than that of CS. When Icorr is less than10^{-7} A/cm^2, it can be considered that the electrode is not corroded or completely passivated [32]. As for TF, the values of Icorr were less than 10^{-7} A/cm^2 in all

passivation ages. It indicates that TF has good passivation performance and can maintain high corrosion resistance in simulated concrete pore solution.

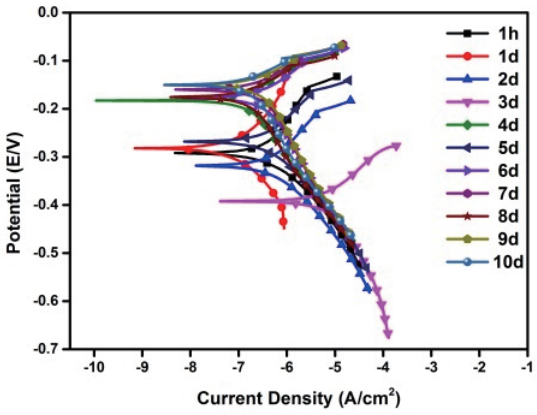

a

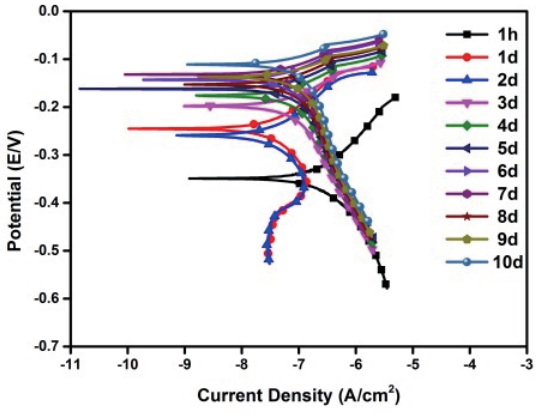

b

Fig. 3 Potentiodynamic polarization curve of working electrodes immersed in simulated concrete pore solution, (a) CS and (b) TF

3.3 Electrochemical impedance spectroscopy of passivation system

Nyquist plots of the impedance spectra were represented in Fig. 4. As can be seen from the Fig. 4, all curves were composed of arcs with various radiuses in the low frequency area. In the high frequency region, it is composed of multiple diagonal lines. Moreover, the semicircle diameter increased as the development of passivation ages at low frequencies (< 1 Hz). It indicates that the resistance value and capacitive reactance value of passive film increased as the extension of soaked ages.

To further study the detailed information about the passive film, the equivalent electric circuit ($R_s(Q_f(R_f(Q_{ct}\ R_{ct})))$) was elected to fit the impedance spectrum data by ZSimpWin software. The equivalent circuit was shown in Fig. 4c. In this equivalent circuit model, R_s is the solution resistance, and representing the conductivity of the passivation solution. Q_f and Rf are on behalf of the capacitance and resistance respectively of passive film. Q_{ct} and Rct are associated with double-layer capacitance and charge transfer resistance of steel bar. During the fitting process, R_s can be ignored due to the high conductivity of the alkaline solution. Besides, R_p can be regarded as the sum of R_{ct} and R_f ($R_p = R_{ct} + R_f$). The results of fitting were shown in table 4. It can be seen from table 4 that with the extension of passivation ages, the R_f values of TF enlarged gradually from 3.2×10^3 Ω.cm^2 to the maximum values of 2.1×10^5 Ω.cm^2, and the R_f values of CS increased from 2.2×10^1 Ω.cm^2 to 2.3×10^4 Ω.cm^2. The values R_f of TF was higher than that of CS at all stages of passivation. It shows that the passivability of TF is superior to that of CS. The C_f is negative correlation to the thickness of passivation film. As the passivation ages extension, the thickness of passivation film enlarged and the C_f decreased. The C_f of TF and C_S increased gradually from 1.1×10^{-3} F/cm^2 and F/cm^2 Ω.cm^2 to the maximum value of 1.2×10^{-6} F/cm^2 and 2.7×10^{-5} F/cm^2. It indicates that the corrosion resistance of the passive film of TF is much better than that of CS.

Table 3. Corrosion current density (Icorr (A/cm2)) and polarization resistance (Rp (Ω.cm^2)) of CS and TS

		1h	1d	2d	3d	4d	5d	6d	7d	8d	9d	10d
TF	Icorr	5.5E-06	6.3E-07	4.4E-07	6.9E-08	5.7E-08	5.0E-08	4.5E-08	2.1E-08	3.2E-08	2.3E-08	1.7E-08
	Rp	2.8E+03	5.8E+04	8.7E+04	5.7E+05	6.5E+05	7.4E+05	8.8E+05	1.6E+06	9.5E+05	1.0E+06	1.9E+06
CS	Icorr	4.9E-04	1.2E-06	5.5E-05	6.6E-05	4.3E-05	3.6E-05	3.7E-06	3.1E-06	3.2E-06	2.3E-06	3.5E-06
	Rp	5.7E+02	2.3E+04	3.3E+03	2.8E+03	4.9E+03	8.2E+03	6.3E+04	6.8E+04	6.1E+04	7.3E+04	6.8E+04

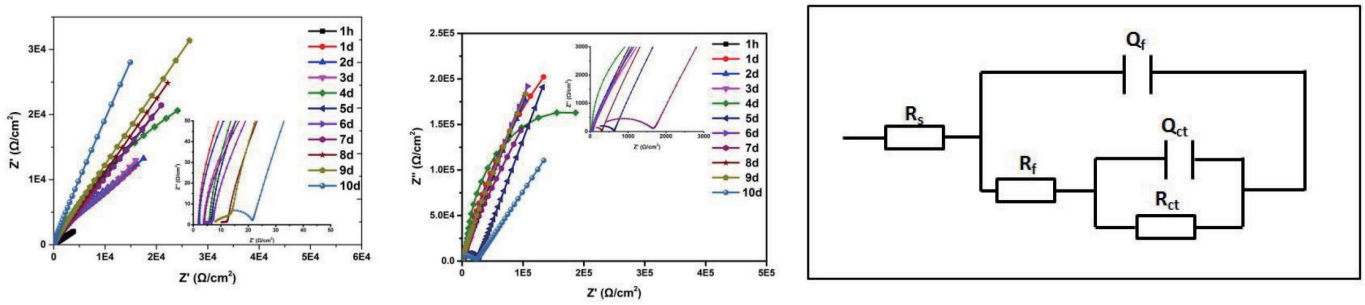

a b c

Fig. 4 EIS of working electrodes immersed in simulated concrete pore solution, (a) CS, (b) TF, (c) the equivalent circuit of for the impedance spectra of specimens in simulated solution

Table 4. Resistance (Rf ($\Omega.cm^2$)) and capacitance (Cf (F/cm^2)) of passive film of CS and TF

		1h	1d	2d	3d	4d	5d	6d	7d	8d	9d	10d
TF	R_f	3.2E+03	3.7E+04	5.9E+04	8.9E+04	1.1E+05	2.6E+05	2.5E+05	2.2E+05	2.1E+05	1.9E+05	2.1E+05
	C_f	1.1E-03	4.7E-04	3.4E-04	9.8E-04	7.6E-05	7.9E-05	6.9E-05	8.1E-05	7.6E-05	6.9E-05	1.2E-06
CS	R_f	2.2E+01	4.9E+02	7.3E+02	7.7E+02	3.5E+03	5.0E+03	9.5E+03	1.6E+04	2.0E+04	2.2E+04	2.3E+04
	C_f	7.3E-03	7.2E-04	5.7E-04	5.2E-04	2.9E-04	1.1E-04	9.3E-05	3.3E-05	3.4E-05	2.6E-05	2.7E-05

3.4 Scanning electron spectroscopy coupled with energy dispersive microscopy

The SEM images with EDS were used to investigate the morphology and elementary composition of the passive film. As for TF, the surfaces were relatively smooth and without obvious scratch (shown in Fig. 5a). It' s because that the scratches on the surface were covered by oxide film. At the same time, some sediment can be seen on the surface. According to EDS diffraction pattern, it can be known that the deposits were calcium hydroxide. The composition of passive film of TF and CS was shown in table.5. The results shows that the oxygen content of TF reached about 24% and that of CS reached about 16%. For CS, the passive film has a double layer structure and with different components. The inner layer is mainly FeO and the outer layer is mainly FeOOH in alkaline solution [33]. However, the passive film of TF has a monolayer structure and thicker than that of carbon steel. As the thickness of passive film changes, the proportion of TiO_2/Ti_2O_3 in passive film component was different [34]. The results of elemental analysis show that the surface of specimens contains around 3% carbon. That attributed to that carbon dioxide in the air dissolves in the alkaline solution and forms a precipitate under highly alkaline conditions.

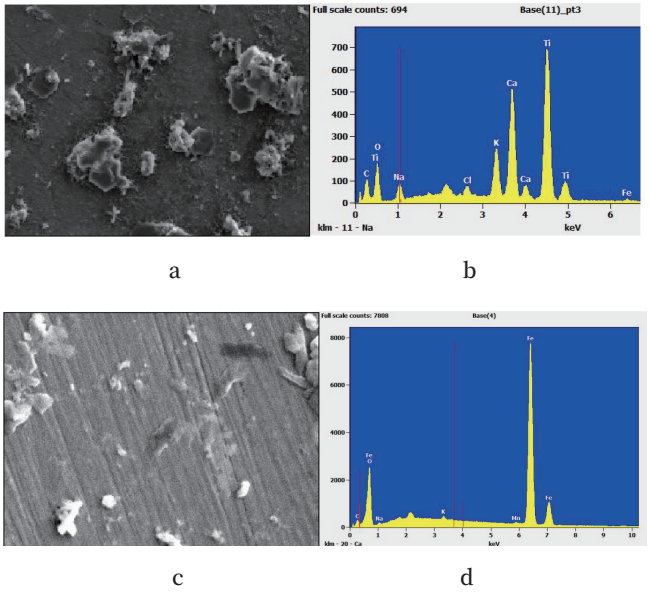

a b

c d

Fig. 5 (a) SEM and (b) EDS analysis for the surfance of TF that was immersed in simulated solution. (c) SEM and (d) EDS analysis for the surfance of CS that was immersed in simulated solution.

Table 5. Element analysis of the surface of TF and CS (wt%)

	C-K	O-K	Na-K	K-K	Ca-K	Ti-K	Fe-K
TF	3.26	23.65	2.56	6.46	17.85	42.97	1.14
CS	2.63	16.16	0.16	0.12	0	0	80.85

3.5 Open circuit potential evolution during corrosion ages

The OCP curves of CS and TF in different corrosion solutions were shown in Fig. 6. It can be seen from Fig.6a that the OCP value of CS reduced from -0.25 V_{SCE} to -0.6 V_{SCE} sharply within 56 days of corrosion in corrosion solution. As for TF, the value of OCP decreased from -0.1 V_{SCE} to -0.42 V_{SCE} within a week of soaking. However, with the corrosion continues, the value of OCP increased from -0.42 V_{SCE} to 0.2 V_{SCE}. That indicates that TF has strong corrosion resistance and secondary passivation performance. Under high chloride concentration condition, the passive film of TF was dissolved firstly and then formed dense passive film again. As shown in Fig 6, the OCP value of CS, which soaking in 7.0 wt% sodium chloride solution, decreased from -0.303 V_{SCE} to -0.633 V_{SCE} for within 56 days of corrosion, and the value of TF first dropped from -0.135 V_{SCE} to -0.36 V_{SCE} y, and then gradually enlarged to -0.05 V_{SCE}. This illustrates that TF showed better chlorine resistance than CS in extreme environments with high chlorine concentrations.

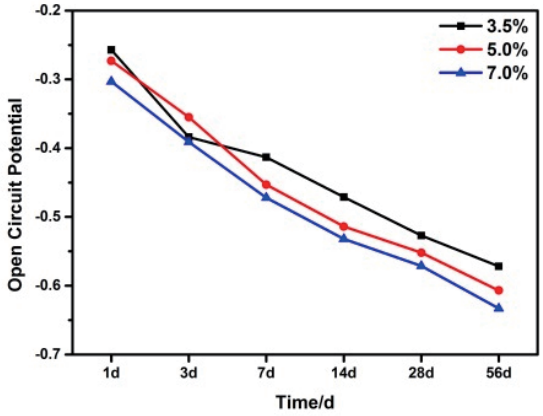

a

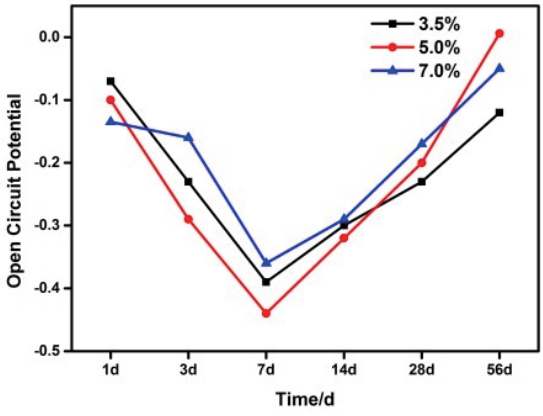

b

Fig. 6 Evolution of open-circuit potential of specimens immersed in corrosion solution. (a) CS, (b) TF

3.6 Potentiodynamic polarization curve of passivation system

The tafel curves of TF and CS, which soaked in corrosion solution, were shown in Fig. 7. At the initial stage of corrosion, the Ecorr of CS and TF were about -0.3 V_{SCE} and -0.1 V_{SCE} respectively. As the corrosion continues, the value of CS dropped from-0.3 V_{SCE} to -0.6 V_{SCE} sharply. From Figs (a) (b) (c) can be seen that the Ecorr value of TF reduced gradually within a week. However, with the prolonging of the corrosion age, the Ecorr enlarged gradually. This may be due to the secondary passivation of TF restored the original passive film. This indicates that TF can tolerate higher concentration of chloride ions than CS.

R_p and Icorr of CS and TF were calculated by linear fitting for the polarization curves, and the results were shown in table.6 and table.7. It can be seen form table.6 that with the extension of corrosion ages, I_{corr} of CS increased from 10^{-7} A/cm^2 to 10^{-4} A/cm^2, and Rp decreased from 10^4Ω.cm^2 to 10^3Ω.cm^2. For example, the Icorr of CS increased from 3.04×10^{-7} A/cm^2 to 1.19×10^{-4} A/cm^2 and R_p decreased from 4.95×10^5Ω.cm^2 to 4.94×10^3Ω.cm^2 in the solution of 5.0% sodium chloride. This indicates that CS has poor corrosion resistance to chlorine under extreme environments.

It can be seen from table 7. that the I_{corr} of TF increased from 5.71×10^{-7} A/cm^2 to 5.23×10^{-6} A/cm^2 within 1d to 7d corrosion ages and the Rp decreased from1.57×10^5 Ω.cm^2 to 7.88×10^4 Ω.cm^2 in the solution of 7.0% sodium chloride. When the corrosion ages range from 7d to 56d, the Icorr of TF reduced from 5.23×10-6 A/cm^2 to 9.29×10^{-7} A/cm^2, and Rp increased from 7.88×10^4 Ω.cm^2 to 1.15×10^5 Ω.cm^2. This shows that TF exhibit excellent stability and corrosion resistance under high concentration of chlorine. TF have strong passivation and secondary passivation properties, and the surface passive film has higher stabilities than CS. The surface of TF will form dense passive film structure again rapidly to maintain high corrosion resistance when the surface passive film was destroyed.

Conclusion

The passivity and corrosion resistance performance of TF and CS solution were investigated in the simulated concrete pore. The OCP values of TF and CS show that the initial passivation tendency is relatively greater under the highly alkaline environment. Not only that, TF can also be passivated in high chlorine concentration. With the extension of passivation ages, the OCP values of CS and TF enlarged from -400 mV~-300 mV to -200 mV~-100 mV gradually, and the R_p increased by about 100 times. The passivation rate of TF is much higher than that of CS steel. For TF, a stable passive film can be formed after 3 days of passivation. While for CS, it takes 6 days to form a stable film. The Icorr of CS is about 3×10^{-6} A/cm^2, and that of TF is 2×10^{-8} A/cm^2 when in a completely passive state.

In chloride environment, CS showed poor corrosion resistance. The passive film dissolved and Icorr increased sharply. The value I_{corr} increased from 10^{-7} A/cm^2 to 10^{-4} A/

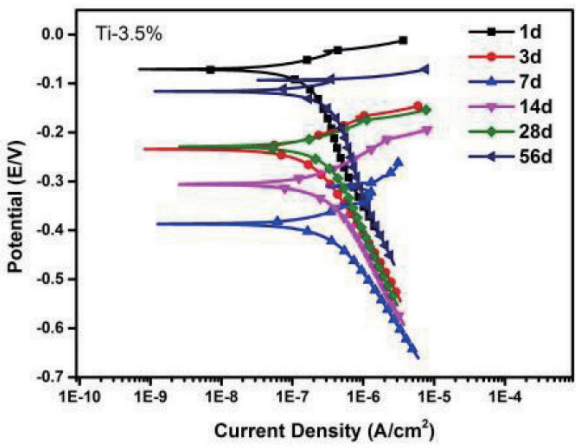

(a)

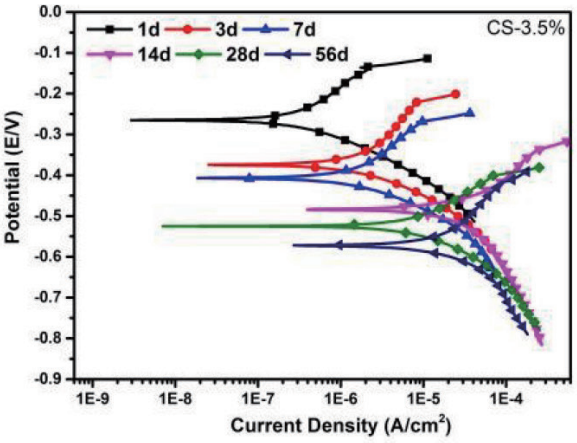

(d)

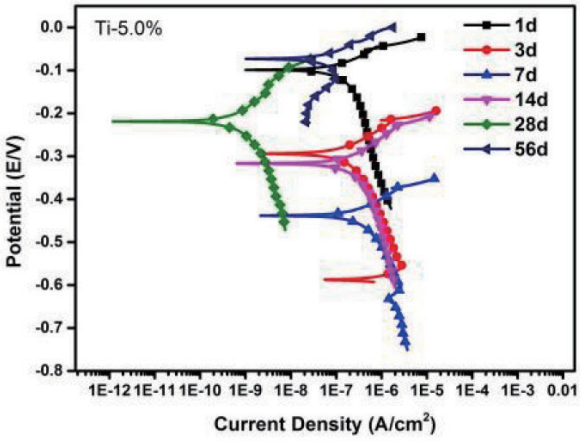

(b)

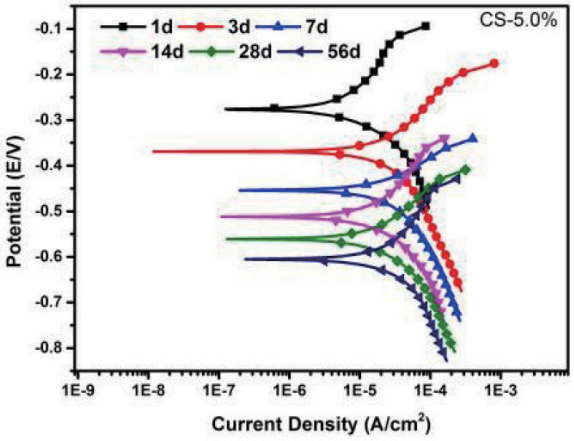

(e)

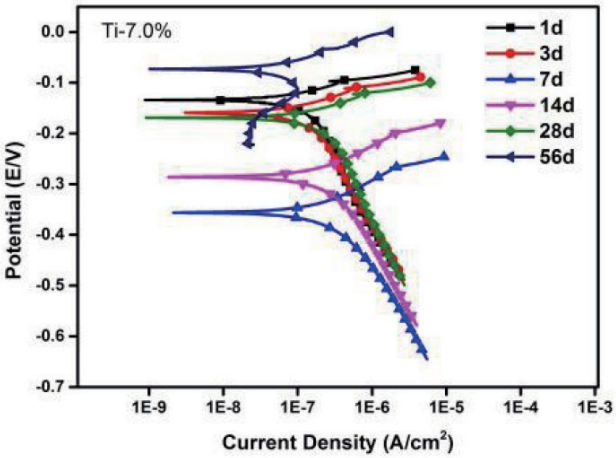

(c)

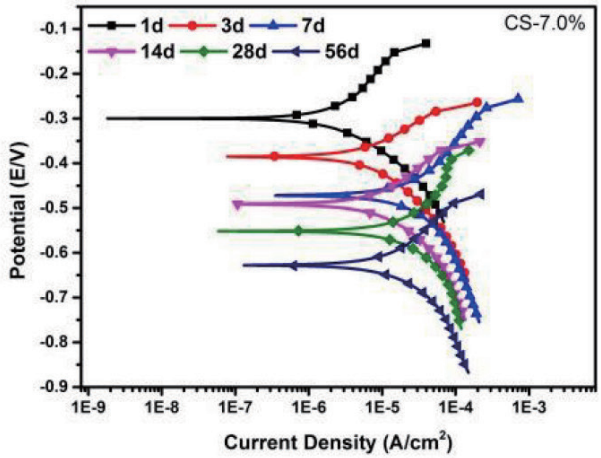

(f)

Fig. 7 Potentiodynamic polarization curve of working electrodes immersed in Corrosion solution; (a) TF- 3.5 wt%, (b) TF- 5.0 wt%, (c) TF- 7.0 wt%, (d) CS- 3.5 wt%, CS- 5.0 wt%, (c) CS- 7.0 wt%.

Table 6. Icorr (A/cm^2) and Rp (Ω.cm^2) of CS in different corrosion solution.

CS		1d	3d	7d	14d	28d	56d
I_{corr}	3.5%	4.07E-07	1.37E-07	2.24E-06	8.94E-06	7.05E-05	9.94E-05
	5.0%	3.04E-07	7.31E-07	4.38E-06	6.28E-06	2.24E-05	1.19E-04
	7.0%	2.94E-07	1.09E-06	1.84E-05	5.36E-05	3.44E-04	8.28E-04
R_p	3.5%	6.32E+04	3.39E+04	1.46E+04	1.17E+04	8.72E+03	6.55E+03
	5.0%	4.95E+04	2.96E+04	1.33E+04	8.53E+03	6.66E+03	4.54E+03
	7.0%	4.11E+04	1.50E+04	1.01E+04	5.87E+03	3.77E+03	1.35E+03

Table 7. Icorr (A/cm^2) and Rp (Ω.cm^2) of TF in different corrosion solution.

TF		1d	3d	7d	14d	28d	56d
I_{corr}	3.5%	1.04E-07	3.27E-07	3.90E-07	2.31E-07	1.37E-07	1.26E-07
	5.0%	1.39E-07	3.77E-07	5.25E-07	2.34E-07	3.64E-08	5.83E-07
	7.0%	5.71E-07	9.91E-07	5.23E-06	2.17E-06	1.40E-06	9.20E-07
R_p	3.5%	1.54E+05	1.33E+05	8.53E+04	1.02E+05	9.71E+04	1.53E+05
	5.0%	1.38E+05	1.18E+05	5.61E+04	9.81E+04	3.73E+05	2.14E+05
	7.0%	1.57E+05	1.27E+05	7.88E+04	8.90E+04	1.08E+05	1.15E+05

cm^2 within two months. Compared with CS, TF shows better corrosion resistance. Under high chloride concentration, TF not only has high corrosion resistance, but also has strong secondary passivation performance. Icorr of TF was maintained at 10^{-7} A/cm^2 and Rp maintained at a high level which about 10^5Ω.cm^2. It showed that TF reinforcing bar may be more suitable for stirrups in aggressive environment, such as marine and deicing salt environments.

In engineering applications, the use of TF - CS composite reinforcing bars can be attempted. Coating the surface of carbon steel with a layer of titanium alloy can not only significantly enhance the corrosion resistance of the steel bars, but also to a certain extent alleviate the high cost problem caused by the use of titanium alloy.

References

[1] Zhu, M. Passivation Behavior of 2507 Super Duplex Stainless Steel in Simulated Concrete Pore Solution.Journal of Materials Engineering and Performance, 2020.

[2] Sánchez-Moreno, M. A theoretical approach of impedance spectroscopy during the passivation of steel in alkaline media. Electrochimica Acta, 2009. 54(28): p. 7222-7226.

[3] Shen F, Li M, Liu G, et al. Unveiling the intricacies of steel corrosion induced by chloride: Insights from reactive molecular dynamics simulation[J]. Construction and Building Materials, 2024, 443: 137839.

[4] Sahoo, G, R. Balasubramaniam. On the corrosion behaviour of phosphoric irons in simulated concrete pore solution. Corrosion Science, 2008. 50(1): p. 131-143.

[5] Feng, X. The influence of strain on the passive behavior of carbon steel in cement extract. Corrosion Science, 2012. 65: p. 542-548.

[6] Ann, K.Y., J.H. Ahn, et al. The importance of chloride content at the concrete surface in assessing the time to corrosion of steel in concrete structures. Construction and Building Materials, 2009. 23(1): p. 239-245.

[7] M. Saremi*, E.M., A study on chloride-induced depassivation of mild steel in simulated concrete pore solution. Cement and Concrete Research, 2002.

[8] Wang, Q. Mechanical properties and microstructure of Portland cement concrete prepared with coral reef sand. Journal of Wuhan University of Technology-Mater. Sci. Ed., 2016. 31(5): p. 996-1001.

[9] J.A. González, J.M.M., N., et al. Electrochemical techniques for studying corrosion of reinforcing steel Limitations and advantages. corrosion Science Section, 2005.

[10] Scully, M.F.H.a.J.R., Threshold Chloride Concentrations of Selected Corrosion Resistant Rebar Materials Compared to Carbon Steel. Corrosion Science Section, 2006.

[11] Liu G, Shen F, Zhang Y, et al. Reactive molecular dynamics study on carbon steel corrosion induced by chloride: Effects of applied potential and temperature[J]. Construction and Building Materials, 2024, 411: 134250.

[12] Ohtsuka T, Nishikata A, et al. Electrochemistry for Corrosion Fundamentals[J]. 2018..

[13] Hamada, E. Direct imaging of native passive film on stainless steel by aberration corrected STEM.Corrosion Science, 2010. 52(12): p. 3851-3854.

[14] Lu, Z. , D.D. Macdonald. Transient growth and thinning of the barrier oxide layer on iron measured by real-time spectroscopic ellipsometry. Electrochimica Acta, 2008. 53(26): p. 7696-7702.
[15] Grosvenor, A.P. Investigation of multiplet splitting of Fe 2p XPS spectra and bonding in iron compounds. Surface and Interface Analysis, 2004. 36(12): p. 1564-1574.
[16] Liu G, Li J, Zhang Y. Corrosion of carbon steels subjected to chloride and sulfate in simulated concrete pore solutions with different pH[J]. Construction and Building Materials, 2024, 440: 137445.
[17] Krishna, N.G. Surface modification of type 304 stainless steel with duplex coatings for corrosion resistance in sea water environments. Surface Engineering, 2014. 31(1): p. 39-47.
[18] Wei, S., Mechanistic Aspects of Factors Affecting Pitting Corrosion of Metallic Materials for Marine Application: A Review Paper. International Journal of Electrochemical Science, 2019: p. 3949-3967.
[19] P., M., Corrosion mechanism in theory and practice. M, 2002.
[20] Gai, X. Electrochemical behaviour of passive film formed on the surface of Ti-6Al-4V alloys fabricated by electron beam melting. Corrosion Science, 2018. 145: p. 80-89.
[21] Chen, R., Characterization of the passive film formed on the reinforcement surface in alkali activated fly ash: Surface analysis and electrochemical evaluation. Corrosion Science, 2020.165.
[22] Milosev, I., T. Kosec et al. Strehblow, XPS and EIS study of the passive film formed on orthopaedic Ti–6Al–7Nb alloy in Hank's physiological solution. Electrochimica Acta, 2008. 53(9): p. 3547-3558.
[23] Vasilescu, C. Surface analysis and corrosion resistance of a new titanium base alloy in simulated body fluids. Corrosion Science, 2012. 65: p. 431-440.
[24] I. Milosev. Passive lm on orthopaedic TiAlV alloy formed in physiological solution investigated by X-ray photoelectron spectroscopy. . Biomaterials, 2000(21 (2000) 2103).
[25] Abreu, C.M. Comparative study of passive films of different stainless steels developed on alkaline medium. Electrochimica Acta, 2004. 49(17-18): p. 3049-3056.
[26] Zhang, Y. Effect of Fe Content on Microstructure Evolution and Mechanical Properties of as-cast Ti-xFe-B Alloy. Rare Metal Materials and Engineering, 2017. 46: p. 180-184.
[27] Guoqing Dai, Yuwen Cui, et al. Hot Deformation Behavior and Mechanistic Understanding of New TF400 Titanium Alloy. 2019, 9(12)
[28] Sánchez, M. Electrochemical impedance spectroscopy for studying passive layers on steel rebars immersed in alkaline solutions simulating concrete pores. Electrochimica Acta, 2007. 52(27): p. 7634-7641.
[29] Dong, Z.*, Fu, C.,et al. Effect of static and dynamic tensile stress changes on carbon steel passivation in alkaline environment. Electrochimica Acta, 538, 2025.
[30] Cai, Y. Comparative studies on passivation and corrosion behaviors of two types of steel bars in simulated concrete pore solution. Construction and Building Materials, 2021. 266.
[31] Farhat Ali, Mazhar Mehmood, et al. Comparative study of the structure and corrosion behavior of Zr-20%Cr and Zr-20%Ti alloy films deposited by multi-arc ion plating technique. 2014, 564:277-283.
[32] Du, F. Chloride ions migration and induced reinforcement corrosion in concrete with cracks: A comparative study of current acceleration and natural marine exposure. Construction and Building Materials, 2020.263.
[33] Oliveira, J.A.M. Effect of current density, temperature and bath pH on properties of Ni–W–Co alloys obtained by electrodeposition. Journal of Alloys and Compounds, 2021. 853.
[34] Chen, Z. Study on the adsorption of OH − and CaOH+ on Fe (100) surface and their effect on passivation of steel bar: Experiments and DFT modelling. Corrosion Science, 2020. 174.
[35] Tian, Y. A comparison study on the natural and half-soaking galvanic accelerated corrosion of reinforced concrete based on an improved electrochemical model. Construction and Building Materials, 2020. 261.